

## BUCKLING STABILITY OF MULTILAYER PLATES AND SHELLS WITH INTERFACIAL STRUCTURAL DEFECTS UNDER AXIAL COMPRESSION

S. M. Vereshchaka

*Keywords: buckling stability, composite, multilayer elements, transverse shear and compression, interfacial defects*

*Based on the discrete-structural theory of thin plates and shells, a variant of the equations of buckling stability, containing a parameter of critical loading, is put forward for the thin-walled elements of a layered structure with a weakened interfacial contact. It is assumed that the transverse shear and compression stresses are equal on the interfaces. Elastic slippage is allowed over the interfaces between adjacent layers. The stability equations include the components of geometrically nonlinear moment subcritical buckling conditions for the compressed thin-walled elements. The buckling of two-layer transversely isotropic plates and cylinders under axial compression is investigated numerically and experimentally. It is found that variations in the kinematic and static contact conditions on the interfaces of layered thin-walled structural members greatly affect the magnitude of critical stresses. In solving test problems, a comparative analysis of the results of stability calculations for anisotropic plates and shells is performed with account of both perfect and weakened contacts between adjacent layers. It is found that the model variant suggested adequately reflects the behavior of layered thin-walled structural elements in calculating their buckling stability.*

### Introduction

In the majority of studies dedicated to the investigation of buckling stability of composites shells, it is assumed that the condition of a perfect contact between their layers [1-3] is satisfied. This assumption is one of the idealizations introduced in the calculation model of layered shells. In practice, as a rule, areas of local adhesion failure and delaminations occur at layer interfaces. In this case, the assumption of continuity of displacements and stresses upon crossing the interfaces can be violated considerably.

The calculation model of shells with delaminations suggested in [4], in which the presence of interlaminar defects is taken into account by modifying the expression for the flexural rigidity, seems to be the simplest one. It is obvious that this model does not allow us to analyze a number of mechanical phenomena that accompany the process of subcritical deformation and buckling of layered structures.

---

Sumy State University, Sumy, Ukraine. Translated from *Mekhanika Kompozitnykh Materialov*, Vol. 43, No. 4, pp. 513-530, July-August, 2007. Original article submitted December 2, 2006; revision submitted March 12, 2007.

A solution to the problem of stability of structural elements with delaminations, with account of local effects, is given in [5, 6], where the effect of the sizes and arrangement of interlaminar defects on the stability of cylindrical and spherical shells is examined. Multilayer shells of revolution with gaps between their layers were considered in [7].

The question on the accuracy of the results of stability calculations for shells with delaminations, obtained under various assumptions, was investigated in [8]. It was found that, in problems on the stability of layered shells with an imperfect contact between layers, the two-dimensional theory led to more serious errors than in the case of heterogeneous shells without defects. A detailed analysis of recent results and trends in the development of stability theory for layered plates and shells can be found in review [9].

In the present study, for modeling the areas of a weakened interfacial contact, a variant of the model of contact problem on the adhesion of rigid anisotropic layers is considered. It is typical of this model variant that the static contact conditions are fulfilled at the interface between individual layers (the first model). The interfacial tangential and normal stresses on the contact boundary are assumed equal. In this case, elastic slippage is allowed over the interface of adjacent layers. If, on some local area of the shell, a glue layer is absent, a unilateral contact between rigid layers is taken into account in this area [10].

The reliability of results obtained by the first model was estimated by using the continuous structural model of the theory of plates and shells (the second model). The second model is well known and is frequently used to calculate anisotropic thin-walled elements, when layered plates or shells, piecewise-inhomogeneous across the thickness, are regarded as quasi-homogeneous with reduced elastic characteristics.

### Statement of the Problem and the Solution Method

It is assumed that the multilayer shell considered consists of  $n$  thin anisotropic layers (Fig. 1). Each layer of the undeformed shell is related to an orthogonal curvilinear coordinate system  $x^i$  ( $i = 1, 2$ ),  $z^{(k)}$ . The  $z^{(k)}$  coordinate is directed along the common normal  $\mathbf{m}^{(k)}$  to the midsurface  $S^{(k)}$  and an equidistant surface  $S_z^{(k)}$ ;  $k$  is the layer number. In introducing new symbols, the subscript “ $z$ ” means that the corresponding quantities refer to a point  $(x^1, x^2, z^{(k)})$  on the equidistant surface  $S_z^{(k)}$ .

The vector of total displacement  $\mathbf{u}_z^{(k)}$  of a point of a rigid layer, according to the refined Timoshenko theory of shells, can be presented in the form

$$\mathbf{u}_z^{(k)} = \mathbf{u}^{(k)} + z^{(k)} \boldsymbol{\omega}^{(k)} + \mathbf{g}^{(k)}(z^{(k)}), \quad (1)$$

where  $\mathbf{u}^{(k)}$  is the displacement vector of points of the midsurface  $S^{(k)}$ ;  $\boldsymbol{\omega}^{(k)}$  is the vector function of rotation angles and compression of the fibers perpendicular to the undeformed midsurface  $S^{(k)}$ ;  $\mathbf{g}^{(k)}(z^{(k)})$  is a nonlinear continuous distribution function of tangential displacements across the layer thickness, whose analysis and approximation are presented in [11];  $\boldsymbol{\omega}^{(k)}(x^1, x^2)$  is the vector function of shear. The covariant components of the vectors  $\mathbf{u}^{(k)}$ ,  $\boldsymbol{\omega}^{(k)}$ , and  $\mathbf{g}^{(k)}$  are given by the expressions

$$\begin{aligned} u_i^{(k)} &= \mathbf{r}^{(k)i} u_i^{(k)} + \mathbf{m}^{(k)w} w^{(k)}, \quad \omega_i^{(k)} = \mathbf{r}^{(k)i} \omega_i^{(k)} + \mathbf{m}^{(k)w} \omega_w^{(k)}, \\ \omega_w^{(k)} &= \mathbf{r}^{(k)i} \omega_i^{(k)}. \end{aligned} \quad (2)$$

The components of the tensor of finite strains at a point  $(x^1, x^2, z^{(k)})$  is determined as half-differences between the components of metric tensors before and after deformation:

$$2 \epsilon_{ij}^{(k)z} = g_{ij}^{(k)} - g_{ij}^{(k)}, \quad 2 \epsilon_{i3}^{(k)z} = g_{i3}^{(k)} - g_{i3}^{(k)}, \quad 2 \epsilon_{33}^{(k)z} = g_{33}^{(k)} - 1. \quad (3)$$

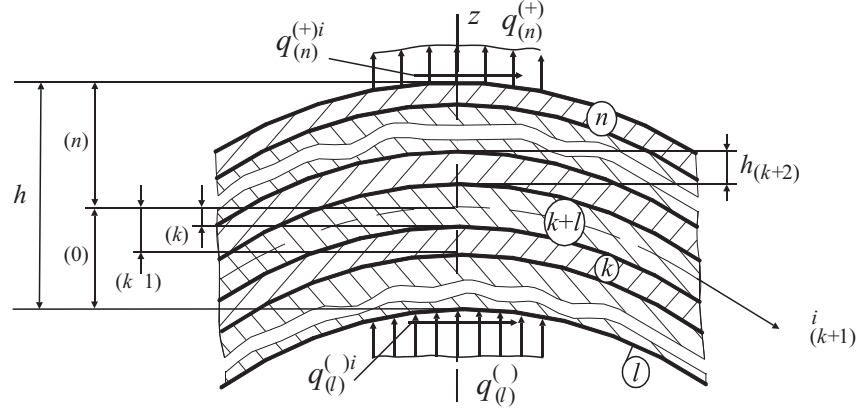


Fig. 1. Structure and designation of layers across the thickness of a thin-walled structural element.

If we assume that the axial lines of the general and local coordinate systems coincide along the normal to the midsurfaces of individual layers of the shell and the local coordinate surfaces coincide with the layer midsurfaces, the Reissner variational equation for the multilayer shell can be written as

$$\int_{k=1}^n \int_{V^{(k)}} ( \sigma_{(k)}^i \epsilon_{(k)}^i - F^{(k)} ) dV = 0 \quad (i, j = 1, 2, 3). \quad (4)$$

The layers are numbered from unity to  $n$ , beginning with negative values of the coordinate;  $F^{(k)}$  is the additional unit work of deformation;  $\sigma_{(k)}^i$  and  $\epsilon_{(k)}^i$  are the components of stress and strain tensors.

If the kinematic and static perfect contact conditions are fulfilled between the adjacent faces of layers

$$u^{(k,k-1)} = u^{(k-1,k)}, \quad X_{(k,k-1)} = X_{(k-1,k)}, \quad (5)$$

the variation of the elementary work of external forces  $A_R$  can be presented in the form

$$\begin{aligned} A_R = & \int_{k=1}^n \int_{S^{(k)}} ( \mathbf{X}_{(k)} \mathbf{u}^{(k)} + M_{(k)}^i \mathbf{r}_i^{(k)} + B_{(k)}^i \mathbf{r}_i^{(k)} ) \\ & M_{(k)}^3 \epsilon_{33}^{(k)} ) dS + \int_{k=1}^n \int_{l_1^{(k)}} ( \sigma_{(k)}^S \mathbf{u}^{(k)} + \mathbf{G}_{(k)}^S + \mathbf{L}_{(k)}^S ) dl \\ & \int_{k=1}^n \int_{l_2^{(k)}} [ \sigma_{(k)}^i \mathbf{u}^{(k)} + G_{(k)}^i + L_{(k)}^i + ( \mathbf{u}^{(k)} \mathbf{u}_S^{(k)} ) ] \\ & ( \sigma_{(k)}^i \epsilon_{(k)}^i + \mathbf{G}_{(k)}^i + ( \mathbf{u}^{(k)} \mathbf{u}_S^{(k)} ) \mathbf{L}_{(k)}^i ] dl. \end{aligned} \quad (6)$$

Here,  $S^{(k)}$  is the layer midsurface;  $l_1^{(k)}$  and  $l_2^{(k)}$  are parts of the contour  $l^{(k)}$ . The vectors of external forces  $\mathbf{X}_{(k)}$ , moments  $\mathbf{M}_{(k)}$ , and additional moments  $\mathbf{B}_{(k)}$ , which enter into Eq. (6), are determined by the equalities



$$\frac{F^{(k)}}{i_3^{(k)}} \quad 2 \quad \frac{(k)z}{i_3^{(k)}} \quad \frac{i_3}{(k)} \quad \frac{F^{(k)}}{33^{(k)}} \quad \frac{(k)z}{33^{(k)}} \quad \frac{33}{(k)} \quad dV \quad (i, j = 1, 2).$$

Inserting geometrical relations (1)-(3) into Eqs. (4), (6), and (9) and using the Reissner variational principle, we readily come to the system of equilibrium equations, the physical relations, and the static and kinematic boundary conditions for each individual layer of the shell. The transition to physical components of the tensors used in this study and the deduction of equilibrium equations and boundary conditions are described in [10].

### Linearized Equations of Stability

The linearized equations of stability of multilayer shells of revolution are derived by using the geometrically nonlinear equations of discrete-structural theory [10] and the Euler static criterion, i.e., mixed equilibrium modes of the compressed structural element, close to the initial one but distinct from it, are allowed. The critical load is defined as the smallest load under which mixed equilibrium modes along with the initial one are possible.

Let the existence of a mixed equilibrium configuration under an external load be determined by the expressions

$$\begin{aligned} & u_i^{(k)0} \quad u_i^{(k)}, \quad w^{(k)0} \quad w^{(k)}, \quad \frac{(k)0}{i} \quad \frac{(k)}{i}, \quad \frac{(k)0}{i} \quad \frac{(k)}{i}, \quad \frac{(k)0}{i} \quad \frac{(k)}{i}, \\ & T_{ii}^{(k)0} \quad T_{ii}^{(k)}, \quad T_{12}^{(k)0} \quad T_{12}^{(k)}, \quad R_{i3}^{(k)0} \quad R_{i3}^{(k)}, \quad M_{ii}^{(k)0} \quad M_{ii}^{(k)}, \quad M_{12}^{(k)0} \quad M_{12}^{(k)}, \\ & L_{ii}^{(k)0} \quad L_{ii}^{(k)}, \quad L_{12}^{(k)0} \quad L_{12}^{(k)}, \quad Q_i^{(k)0} \quad Q_i^{(k)}, \quad Q_3^{(k)0} \quad Q_3^{(k)} \quad (i = 1, 2). \end{aligned} \quad (10)$$

Here, the components of the initial subcritical stress-strain state are marked by the superscript “0”, while the additional components of displacements and forces of the perturbed state are given without any superscript.

After substituting Eqs. (10) into the equilibrium equations given in [10] and subtracting the equilibrium equations of initial state from the resulting relations, the linearized stability equations of a  $k$ th layer of the multilayer shell, which include the strains of transverse shear and compression, take the form

$$\begin{aligned} & \frac{(B^{(k)}T_{11}^{(k)})}{(k)_1} \quad \frac{(A^{(k)}T_{12}^{(k)})}{(k)_2} \quad T_{12}^{(k)} \quad \frac{A^{(k)}}{(k)_2} \\ & T_{22}^{(k)} \quad \frac{B^{(k)}}{(k)_1} \quad A^{(k)}B^{(k)}k_1^{(k)}R_{13}^{(k)} \quad 0 \quad (1 \quad 2; A^{(k)} \quad B^{(k)}), \\ & \frac{(B^{(k)}R_{13}^{(k)})}{(k)_1} \quad \frac{(A^{(k)}R_{23}^{(k)})}{(k)_2} \quad A^{(k)}B^{(k)}(k_1^{(k)}T_{11}^{(k)} \quad k_2^{(k)}T_{22}^{(k)}) \quad 0, \\ & \frac{(B^{(k)}M_{11}^{(k)})}{(k)_1} \quad \frac{(A^{(k)}M_{12}^{(k)})}{(k)_2} \quad M_{12}^{(k)} \quad \frac{A^{(k)}}{(k)_2} \quad M_{22}^{(k)} \quad \frac{B^{(k)}}{(k)_1} \\ & A^{(k)}B^{(k)}(R_{13}^{(k)} \quad T_{11}^{(k)0} \quad \frac{(k)}{1} \quad T_{12}^{(k)} \quad \frac{(k)}{2}) \\ & T_{11}^{(k)} \quad \frac{(k)0}{1} \quad T_{12}^{(k)} \quad \frac{(k)0}{2}) \quad 0 \quad (1 \quad 2; A^{(k)} \quad B^{(k)}), \end{aligned} \quad (11)$$

$$\begin{pmatrix} (B^{(k)}L_{11}^{(k)}) \\ (k) \\ 1 \end{pmatrix} \quad \begin{pmatrix} (A^{(k)}L_{12}^{(k)}) \\ (k) \\ 2 \end{pmatrix} \quad L_{12}^{(k)} \quad \begin{pmatrix} A^{(k)} \\ (k) \\ 2 \end{pmatrix} \quad L_{22}^{(k)} \quad \begin{pmatrix} B^{(k)} \\ (k) \\ 1 \end{pmatrix}$$

$$A^{(k)}B^{(k)}L_{13}^{(k)} \quad 0 \quad (1 \quad 2; A^{(k)} \quad B^{(k)}).$$

If the transverse compression of the  $k$ th layer is taken into account, system (11) is supplemented with the eighth equation

$$\begin{pmatrix} (B^{(k)}M_{13}^{(k)}) \\ (k) \\ 1 \end{pmatrix} \quad \begin{pmatrix} (A^{(k)}M_{23}^{(k)}) \\ (k) \\ 2 \end{pmatrix} \quad A^{(k)}B^{(k)}(k_1^{(k)}M_{11}^{(k)} \quad k_2^{(k)}M_{22}^{(k)} \\ k_1^{(k)}L_{11}^{(k)} \quad k_2^{(k)}L_{22}^{(k)} \quad Q_3^{(k)}) \quad 0. \quad (12)$$

Similar to Eqs. (9) and (10), the geometrical relations are also linearized [10]:

$$\begin{matrix} 2 & (k) & e_{ij}^{(k)} & e_{ji}^{(k)} & (k) & (k)0 \\ & ij & & & i & j \end{matrix},$$

$$\begin{matrix} 2 & (k) & i & j & j & i & \sigma_i^{(k)} & e_j^{(k)} & \sigma_j^{(k)} & e_i^{(k)}, \\ & ij & & & & & & & & \end{matrix} \quad (13)$$

$$\begin{matrix} 2 & (k) & 2 & (k) & (k) & (z) & (k) & (k)z & (k) \\ & i3 & & i3 & & i & & 33 & \end{matrix}.$$

Equations (11) and (12) have to be supplemented with the boundary conditions of fastening of contours of the plates or shells considered.

In deducing Eqs. (11) and (12), the additional displacements  $u_i^{(k)}$  and  $w^{(k)}$  were considered small, which allowed us to disregard the degrees of these quantities exceeding the first one. Therefore, based on the resulting system of equations, it is possible to find only the upper critical loads. If a momentless subcritical state is assumed, the underlined terms in the fourth and fifth equations of (11) turn to zero.

Based on the linearized equations of stability (11) and (12), geometrical relations (13), physical relations, and given boundary conditions, a resolving system of 14 homogeneous partial differential equations is derived for a  $k$ th layer of the shell:

$$\frac{\mathbf{Y}^{(k)}}{A^{(k)} \begin{pmatrix} (k) \\ 1 \end{pmatrix}} \quad F \quad \begin{pmatrix} (k) \\ 1 \end{pmatrix}, \begin{pmatrix} (k) \\ 2 \end{pmatrix}, \mathbf{Y}^{(k)}, \frac{\mathbf{Y}^{(k)}}{B^{(k)} \begin{pmatrix} (k) \\ 2 \end{pmatrix}}, \quad k = 1, 2, \dots, n, \quad (14)$$

where

$$\mathbf{Y}^{(k)} = \{Y_1^{(k)}, Y_2^{(k)}, \dots, Y_{14}^{(k)}\}^T = \{T_{11}^{(k)}, T_{12}^{(k)}, R_{13}^{(k)}, M_{11}^{(k)}, M_{12}^{(k)}, L_{11}^{(k)}, L_{12}^{(k)}, \\ u_1^{(k)}, u_2^{(k)}, w^{(k)}, \begin{pmatrix} (k) \\ 1 \end{pmatrix}, \begin{pmatrix} (k) \\ 2 \end{pmatrix}, \begin{pmatrix} (k) \\ 1 \end{pmatrix}, \begin{pmatrix} (k) \\ 2 \end{pmatrix}\}^T$$

is the solution vector.

If we assume that the physicomechanical and geometrical characteristics of the shells of revolution do not vary along the  $z$  coordinate, the solution of resolving equations (14) of the stability problem can be presented in the form of Fourier series

$$\mathbf{Y}_1^{(k)} = \mathbf{Y}_{1,n}^{(k)} \cos n z, \quad \mathbf{Y}_2^{(k)} = \mathbf{Y}_{2,n}^{(k)} \sin n z, \quad (15)$$

where

$$\mathbf{Y}_1^{(k)} = \{T_{11}^{(k)}, T_{22}^{(k)}, R_{13}^{(k)}, Q_1^{(k)}, M_{11}^{(k)}, M_{22}^{(k)}, L_{11}^{(k)}, L_{22}^{(k)}, Q_3^{(k)}, u_1^{(k)}, w_1^{(k)}, y_{1,1}^{(k)}, y_{1,2}^{(k)}, y_{1,11}^{(k)}, y_{1,22}^{(k)}, y_{1,33}^{(k)}, z_{11}^{(k)}, z_{1,22}^{(k)}, z_{1,11}^{(k)}, z_{1,22}^{(k)}\}^T, \quad (16)$$

$$\mathbf{Y}_2^{(k)} = \{T_{12}^{(k)}, R_{23}^{(k)}, Q_2^{(k)}, M_{12}^{(k)}, L_{12}^{(k)}, L_{13}^{(k)}, L_{23}^{(k)}, u_2^{(k)}, z_{2,2}^{(k)}, z_{2,2}^{(k)}, z_{2,12}^{(k)}, z_{2,12}^{(k)}, z_{2,12}^{(k)}\}^T.$$

By substituting Eqs. (15) and (16) into the system of equations (13), we come to the system of ordinary homogeneous differential equations

$$\frac{d\mathbf{Y}_n^{(k)}}{A^{(k)} dz} = F_n^{(k)}(z, n, \mathbf{Y}_n^{(k)}), \quad k = 1, 2, \dots, n, \quad (17)$$

where

$$\mathbf{Y}^{(k)} = \{Y_{1,n}^{(k)}, Y_{2,n}^{(k)}, \dots, Y_{14,n}^{(k)}\}^T = \{T_{11,n}^{(k)}, T_{12,n}^{(k)}, R_{13,n}^{(k)}, M_{11,n}^{(k)}, M_{12,n}^{(k)}, L_{11,n}^{(k)}, L_{12,n}^{(k)}, u_{1,n}^{(k)}, u_{2,n}^{(k)}, w_n^{(k)}, z_{1,n}^{(k)}, z_{2,n}^{(k)}, z_{1,n}^{(k)}, z_{2,n}^{(k)}\}^T$$

is the solution vector. Such a system for a  $k$ th layer of the shell is of 14-th order.

The boundary conditions, which define the fastening conditions for the edges of the  $k$ th layer of the shell, can be presented in the matrix form

$$B_0^{(k)} \mathbf{Y}^{(k)}(z=0) = 0, \quad B_n^{(k)} \mathbf{Y}^{(k)}(z=1) = 0, \quad (18)$$

where  $B_0^{(k)}$  and  $B_n^{(k)}$  are rectangular  $7 \times 14$  matrices.

A stable computation process for the numerical solution of boundary problem (17), (18) is provided by the Godunov method of orthogonal sweep. Integrating the equations presented, we obtain a system of seven algebraic equations in components of the vector of arbitrary constants  $\mathbf{C}^{(k)}$ :

$$B_n^{(k)} Z(z=1, \lambda) \mathbf{C}^{(k)} = 0.$$

Here,  $Z(z=1, \lambda)$  is a  $7 \times 7$  matrix, whose coefficients are obtained by orthogonalization and normalization of the system of solution vectors at each step of numerical integration;  $\lambda$  is an eigenvalue.

For the existence of a nontrivial solution to the problem of stability (17), (18), the condition

$$\left| B_n^{(k)} Z(z=1, \lambda) \right| = 0 \quad (19)$$

must be fulfilled, wherefrom the eigenvalue of the problem is determined. The value of  $\lambda$  is found by using the trial-and-error method until determinant (19) changes its sign for two subsequent iterations of  $\lambda$ .

In constructing the resolving system of stability equations for a shell consisting of two and more rigid layers, the static and kinematic contact conditions on the conjugated surfaces of each layer must be taken into account.

The kinematic and static conditions of perfect contact between the separate layers of thin-walled elements on the conjugated faces have the form

$$2u_i^{(k)} - u_i^{(k-1)} - u_i^{(k+1)} - \frac{h^{(k-1)}}{2} \epsilon_i^{(k-1)} - \frac{h^{(k+1)}}{2} \epsilon_i^{(k+1)} - \frac{h^{(k-1)}}{2} \epsilon_i^{(k-1)} - \frac{h^{(k+1)}}{2} \epsilon_i^{(k+1)} \quad (i = 1, 2), \quad (20)$$

$$2w_{i3}^{(k)} - w_{i3}^{(k-1)} - w_{i3}^{(k+1)} - \frac{h^{(k-1)}}{2} \epsilon_{i3}^{(k-1)} - \frac{h^{(k+1)}}{2} \epsilon_{i3}^{(k+1)}, \quad (i = 1, 2), \quad (21)$$

$$\epsilon_{33}^{(k)} - \epsilon_{33}^{(k-1)}, \quad \epsilon_{33}^{(k)} - \epsilon_{33}^{(k+1)}.$$

Satisfying the kinematic (20) and static (21) contact conditions at the interfaces by means of the penalty function method, we readily set up the complete system of resolving equations (17) for solving the contact problem of the discrete-structural theory of multilayer shells.

Since a soft interfacial glue layer (whose thickness, as a rule, is considered equal to zero) is formed between the rigid layers during the manufacture of multilayer shells, an elastic slippage between the rigid layers is allowed in the model variant suggested, i.e., on the conjugated faces, only static contact conditions (21) are satisfied.

The system of equations (11) includes the forces  $T_{11}^{(k)0}$ ,  $T_{12}^{(k)0}$ , and  $T_{22}^{(k)0}$ , as well as the displacements and shear strains in the coordinate surface of a  $k$ th layer  $u_2^{(k)0}$ ,  $w_{(k)1}^0$ ,  $\epsilon_1^{(k)0}$ , and  $2\epsilon_{13}^{(k)0}$ , which determine the subcritical stress-strain state [10].

A comparison between the systems of resolving equilibrium equations [10] and stability equations (17) shows that they are similar, which allows us to construct a unified computation process for determining the stresses and strains of the non-linear moment subcritical state of shells of revolution and for calculating the critical parameters of external loads.

If we assume that the kinematic bonds between shell layers are absent, unknown force vectors  $\mathbf{q}^{(k)}$  and  $\mathbf{q}^{(k-1)}$  of contact interaction may arise at the interfaces  $S_z^{(k,k-1)}$ . According to Newton's third law,  $\mathbf{q}^{(k)} = -\mathbf{q}^{(k-1)}$ . To take into account the effect of the forces of contact interaction between the layers, Reissner variational equation (4) must be supplied with a term considering the work done by the contact forces acting through the displacement vector of each layer of the section of contact surface:

$$A_q = \int_{m-1}^{n-1} \int_{S_z^{(m,m-1)}} \mathbf{q}^{(m)} \mathbf{u}_z^{(m)} dS.$$

The forces of contact interaction  $\mathbf{q}^{(k)} = q_{(k)}^i \mathbf{r}_i^{(k)} - q_{(k)}^3 \mathbf{m}^{(k)}$  arise if the condition

$$(\mathbf{u}_z^{(k)} - \mathbf{u}_z^{(k-1)}) \cdot \mathbf{0} \quad (22)$$



TABLE 1. Values of Critical Force  $P_{cr}$  for GFRP plates in Axial Compression

Variant of a plate	$L$	$b \cdot 10$	$h \cdot 10^2$	$b/h$	$P_{cr}$ , kN				
	m				Classical theory	Model 2	, %	Model 1	, %
1	0.2	0.51	0.16	31.88	17.77	15.22	14	13.85	22
2	0.2	0.51	0.21	24.29	40.01	35.48	11	27.54	31
3	0.2	0.51	0.26	19.62	71.12	61.22	14	43.67	39
4	0.31	0.76	0.16	47.5	12.62	11.55	8	9.56	24

is satisfied in contact zones between the rigid layers. If inequality (22) does not hold upon displacement of points of the region  $S_z^{(k,k-1)}$  during deformation, the contact pressure  $\mathbf{q}_{(k)}$  in equilibrium equations [10] takes the value  $\mathbf{q}_{(k)} = 0$ . By solving the system of equations [10], it is easy to find, with a given accuracy, the contact pressure of subcritical state by using the iterative method suggested in [7].

### Analysis of Theoretical and Experimental Results

To illustrate the efficiency of the model of multilayer shells and plates suggested, we examined  $[\pm 45/0_3/90]_s$  carbon-fiber-reinforced plastic (CFRP) plates [12], with an epoxy resin as a binder and 60% fibers by volume. The plate was compressed along the longitudinal axis. Assuming that the longitudinal edges are hinge-supported, i.e., at  $y=0$  and  $y=b$ , we have for a  $k$ th layer of the plate

$$u_1^{(k)} \quad w^{(k)} \quad T_{22}^{(k)} \quad M_{22}^{(k)} \quad L_{22}^{(k)} = 0. \quad (23)$$

For the other two edges of the plate, an arbitrary fastening is admitted. The solution to system (17), (18) with account of Eq. (23), has the form

$$\mathbf{Y}_1^{(k)} = \mathbf{Y}_{1,n} \sin \frac{n \cdot y}{b}, \quad \mathbf{Y}_2^{(k)} = \mathbf{Y}_{2,n} \cos \frac{n \cdot y}{b}, \quad (24)$$

where

$$\begin{aligned} \mathbf{Y}_{1,n} &= \{T_{22}^{(k)}, M_{22}^{(k)}, L_{22}^{(k)}, u_1^{(k)}, w^{(k)}\}^T, \\ \mathbf{Y}_{2,n} &= \{T_{11}^{(k)}, T_{12}^{(k)}, R_{13}^{(k)}, R_{23}^{(k)}, Q_1^{(k)}, Q_2^{(k)}, M_{11}^{(k)}, M_{12}^{(k)}, L_{11}^{(k)}, L_{12}^{(k)}, Q_3^{(k)}, \\ &L_{13}^{(k)}, L_{23}^{(k)}, u_2^{(k)}, v_1^{(k)}, v_2^{(k)}, w_1^{(k)}, w_2^{(k)}\}^T. \end{aligned}$$

The right-hand side of resolving equations (17) must be rewritten with regard for expressions (24) and zero values of the layer curvature  $k_1^{(k)} = k_2^{(k)} = 0$  and  $\theta_1^{(k)} = 0$ . A comparison of the results obtained is presented in Table 1.

As expected, the theoretical values of the critical force  $P_{cr}$ , presented in Table 1 and obtained by using the continuously structural theory (model 2) for plates with a low rigidity in transverse shear, are always smaller than those found according to the classical theory, i.e., disregarding the deformations of transverse shear and compression [12]. The difference between the results given by the classical theory and the variant of the refined theory suggested is 8-14%. A noticeable decrease in  $P_{cr}$  (22-39%), compared with the results of classical theory, is observed in calculations based on model 1. This distinction is ex-

TABLE 2. Values of  $P_{cr}$  for Cylindrical GFRP Shells in Axial Compression

Type of structure	Structure	$L/R$	Buckling mode							
			Axisymmetric			Nonaxisymmetric				
			Classical theory	Model 2		Model 2			Model 1	
				MLSS	MSS	Classical theory	MLSS	MSS	MLSS	MSS
1	[0/45/0]	1	80.03	74,08	73,82	40.01(10)	35,23(12)	33,79(12)	14,68(11)	14,62(11)
		2	80.03	74,24	74,01	40.63(8)	35,88(12)	34,23(12)	15,08(10)	15,00(10)
		4	80.03	74.24	74.01	39.82(6)	35.01(10)	33.72(10)	14.01(9)	13.98(9)
2	[45/0/ 45]	1	51.01	50.01	46.28	52.38(1)	49.47(3)	49.47(3)	17.08(10)	17.01(10)
		2	51.01	50.37	46.79	52.38(1)	49.65(3)	49.65(3)	17.59(9)	17.34(9)
		4	51.01	50.37	46.63	52.38(1)	49.02(3)	49.02(3)	17.18(8)	17.01(8)
3	[45/90/ 45]	1	75.95	69.18	68.13	62.04(10)	56.49(8)	56.58(9)	18.46(9)	18.12(9)
		2	75.95	68.61	67.65	61.68(6)	55.71(7)	53.69(7)	18.98(8)	18.76(8)
		4	75.95	68.02	67.54	52.88(4)	52.14(5)	51.07(5)	18.41(7)	18.41(7)
4	[90/45/ 90]	1	49.56	48.84	46.36	40.63(10)	43.14(14)	37.05(15)	15.83(10)	15.66(10)
		2	49.56	48.44	46.83	40.63(10)	43.14(14)	37.05(15)	15.83(10)	15.66(10)
		4	49.56	48,44	46.42	40.63(10)	43.14(14)	37.05(15)	15.41(10)	15.32(10)
5	[90/0/ 90]	1	57.92	55.01	52.16	28.57(11)	18.53(11)	18.53(11)	14.7(9)	14.45(9)
		2	57.92	54.71	51.68	28.57(11)	18.29(10)	18.03(10)	14.91(9)	14.62(9)
		4	57.92	54.71	51.43	28.57(11)	18.01(10)	17.73(9)	14.88(8)	14.43(8)
6	[0/90/ 0]	1	138.6	137.3	125.0	28.51(10)	18.77(7)	18.56(7)	14.47(10)	14.36(10)
		2	138.6	137.1	125.6	28.51(10)	18.71(6)	18.43(6)	14.38(9)	14.01(9)
		4	138.6	137.1	125.5	28.51(10)	18.64(6)	18.21(6)	14.26(8)	14.14(8)

plained by the noticeable decrease in the flexural modulus of the plate upon introduction of the assumptions of model 1. The plate included two rigid anisotropic layers of identical thickness, with weakened contact conditions on the adjacent faces. It is well known that, in most cases where a layered composite structural element is subjected to uniaxial tension or compression, first the polymer matrix fails in the weak layers, as a result of which the rigidity of the element decreases. This statement is once again confirmed by comparing the magnitude of  $P_{cr}$  (the next to the last column in Table 1) obtained from model 1 and the experimental data given in [12]. The difference does not exceed 13%. In a similar comparison between the results of classical theory and experiments [12], the above-mentioned difference varied from 15 to 70% with increasing thickness of the plate.

The efficiency of the variant of calculation model suggested in solving stability problems for compressed cylindrical shells was estimated on the test example given in [13]. Three-layer shells made of a CFRP having a symmetric structure with thickness of each layer  $h = 0.2 \cdot 10^{-3}$  m were examined. The shells had different angles of layer reinforcement: 0, 45, and 90°. Six types of shells with different reinforcement structure were investigated (Table 2). The radius of the shells was  $R = 0.1$  m and the length  $L = (1, 2, 4)R$ . The fibers and matrix had the following physicomechanical characteristics:  $E_f = 4.2 \cdot 10^5$  MPa,  $E_m = 3.5 \cdot 10^3$  MPa,  $\nu_f = 0.21$ , and  $\nu_m = 0.35$ . The volumetric content of carbon fibers was 40%. Other parameters of CFRP were determined according to the dependences suggested in [11].

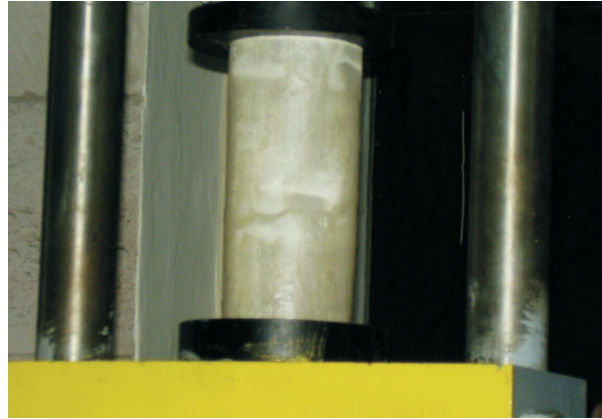


Fig. 2. Buckling mode of a GFRP cylinder.

TABLE 3. Values of  $P_{cr}$  for Cylindrical GFRP Specimens with Hinge-Supported Edges

Specimen	$L$	$R/10$	$L/R$	$h \cdot 10^2, \text{ m}$	$R/h$	$P_{cr}, \text{ kN}$				
	m					Experiment	Model 2	,%	Model 1	,,%
A1	0.1	0.45	2.22	0.10	45.00	14.24	18.66(6)	31	13.57(6)	5
A2	0.1	0.45	2.22	0.11	40.91	15.45	19.86(6)	29	14.07(6)	9
A3	0.1	0.45	2.22	0.10	45.00	13.01	18.88(6)	45	13.57(6)	4
B1	0.2	0.45	4.44	0.10	45.00	14.87	18.66(6)	25	13.57(7)	9
B2	0.2	0.45	4.44	0.11	40.91	16.67	19.86(6)	19	14.07(7)	16
B3	0.2	0.45	4.44	0.10	45.00	15.13	18.66(6)	23	13.57(7)	10
C1	0.1	0.45	2.22	0.20	22.50	48.45	69.15(3)	43	49.46(3)	2
C2	0.1	0.45	2.22	0.21	21.43	50.15	71.03(3)	42	50.87(3)	1
C3	0.1	0.45	2.22	0.20	22.50	47.43	69.15(3)	46	49.46(3)	4
D1	0.2	0.45	4.44	0.20	22.50	45.93	67.85(4)	48	47.46(6)	3
D2	0.2	0.45	4.44	0.22	20.45	46.07	68.09(4)	48	48.17(6)	5
D3	0.2	0.45	4.44	0.20	22.50	46.59	67.85(4)	46	47.46(6)	2

The critical forces  $P_{cr}$  of initial buckling of the cylinders under axial compression, with hinge-supported ends, are given in Table 2. Similar to the previous example, two variants of the calculation model for anisotropic elements were investigated. The influence of the nonlinear moment subcritical state (MSS), as well as the transverse shear and compression strains, on the critical load of the cylinders was considered. For comparison, the results for the shells in the case of a momentless subcritical state (MLSS) are also given in the table.

An analysis of the data given in Table 2 shows that the buckling mode of the structural elements considered, except for model 2 of the cylinder with the second-type structure, is nonaxisymmetric (the number  $n$  of waves in the circumferential direction at the instant of buckling is given in parentheses). In this case, the results obtained according to the second calculation model, in many respects, are determined by the reinforcement direction in the individual layers of the cylinder. Thus, for example, the value of  $P_{cr}$  for the shell with the third-type structure is more than 2.5 times higher than for that with the sixth-type one. The data obtained by using calculation model 1 depend on the type of reinforcement structure only slightly and differ from each other by no more than 25%, which qualitatively agrees with the conclusions drawn in [14, 15]. When the weakened contact be-

TABLE 4. Values of  $P_{cr}$  for Cylindrical GFRP Specimens with Areas of Local Adhesion Failure

Specimen	$L$	$R/10$	$L/R$	$h \cdot 10^2, \text{ m}$	$R/h$	I	$P_{cr}, \text{ kN}$				
	m						Experiment	Model 1			
								II	,%	III	,,%
G1	0.1	0.45	2.22	0.20	22.50	0.05	24.54	26.29(0)	10	36.48(5)	49
G2	0.1	0.45	2.22	0.21	22.43	0.05	25.73	27.01(0)	5	37.12(5)	44
G3	0.1	0.45	2.22	0.20	22.50	0.05	25.04	26.29(0)	5	36.48(5)	46
J1	0.2	0.45	4.44	0.20	22.50	0.16	29.92	26.29(0)	12	30.12(3)	1
J2	0.2	0.45	4.44	0.21	22.43	0.16	30.82	27.01(0)	12	31.28(3)	1
J3	0.2	0.45	4.44	0.20	22.50	0.16	28.68	26.29(0)	8	30.12(3)	5
F1	0.1	0.45	2.20	0.20	22.50	0.08	34.56	26.29(0)	24	36.48(5)	6
F2	0.1	0.45	2.22	0.21	21.43	0.08	35.12	27.01(0)	23	37.12(5)	6
F3	0.1	0.45	2.22	0.20	22.50	0.08	33.36	26.29(0)	21	36.48(5)	9

Note. I is the length of adhesion failure in m; II refers to the local buckling of the external layer; III refers to the total loss of stability.

tween the rigid layers of the anisotropic shell is taken into account, the critical load decreases noticeably in comparison with that obtained from the continuous structural theory.

During the deformation of layered structures in axial compression, the material structure can undergo some changes, i.e., the conditions of perfect contact at the interfaces between adjacent rigid layers can be violated. Therefore, the idealization of the model of multilayer structures according to the classical theory and abandoning the discrete-structural theory, as a rule, yields results differing from experimental data noticeably.

Based on the variant of the calculation model suggested, theoretical and experimental investigations into the stability of cylindrical glass-fiber-reinforced plastic (GFRP) specimens of length 0.1-0.2 m, diameter 0.09 m, and thickness 0.001-0.002 m were carried out. The cylinders consisted of two or four layers of a TG 430-C (100) fiber-glass fabric (Latvia). As a binder, we used a Cistic 2-446 PA polyester orthophthalic resin with a lowered emission of styrene (Great Britain). Some part of the specimens had initial defects in the form of circular local areas of adhesion failure located at the center of the cylinders between their second and third layers. These areas were created while manufacturing the specimens by inserting a thin polyethylene film.

The physicomechanical characteristics of the cylindrical GFRP shells were determined in the following sequence. First, according to GOST 25.601-80, we found the elastic modulus and Poisson ratio of GFRP specimens in compression. The mechanical tests performed allowed us to assert that the material of the specimens could be considered transversely isotropic ( $E_{11} = E_{22} = 1.2 \cdot 10^4 \text{ MPa}$  and  $\nu_{12} = \nu_{21} = 0.12$ ). The other physicomechanical characteristics of the GFRP were determined integrally for the whole package of layers based on the dependences given in [11], where the elastic moduli of the first kind and the Poisson ratios of the fibers and matrices were as follows:  $E_f = 7.0 \cdot 10^4 \text{ MPa}$ ,  $E_m = 3.5 \cdot 10^3 \text{ MPa}$ ,  $\nu_f = 0.22$ , and  $\nu_m = 0.35$ .

The critical buckling loads of the cylindrical specimens with hinge-supported edges are presented in Tables 3 and 4 (the number  $n$  of waves in the circumferential direction is given in parentheses).

The general view of the test plant and the buckling mode of a cylinder of length  $L = 0.2 \text{ m}$  in axial compression are shown in Fig. 2.

A comparison between the theoretical and experimental results allows us to conclude that model 1 (Table 3) of the discrete-structural theory of layered plates and shells rather accurately reflects the deformation process and the behavior of

thin-walled structural elements made of composite materials. The discrepancy between the theoretical and experimental results does not exceed 16%. For model 2, the discrepancy lies within the range of 19-48%. It is seen from the table that, with increasing thickness of the shells, the difference between the experimental value of critical load and that obtained from model 2 grows markedly. We should note that, in testing the defectless cylindrical GFRP specimens, the joint work of layers was observed up to the loss of stability. In this case, as stated theoretically and confirmed experimentally (see Fig. 2), a nonaxisymmetric buckling mode took place.

A somewhat different result was obtained in investigating the size effect of the circular area of adhesion failure at the center of the cylindrical shells on their critical force (Table 3). At a ratio between the length of this area and the cylinder length  $l_{af}/L = 0.5$ , a local axisymmetric buckling of the external layer of the shell occurred in the zone of adhesion failure. At  $l_{af}/L = 0.5$ , both a local axisymmetric buckling of the external layer and a nonaxisymmetric joint buckling of all layers in the zone are possible.

## Conclusions

In the present study, based on the geometrically nonlinear discrete-structural theory of layered structural elements, the stability of anisotropic plates and shells with structural defects of the material was investigated. The interaction of rigid anisotropic layers at their interfaces was described by using two calculation models, with perfect or weakened contact conditions, respectively. The critical forces of two-layer plates and cylindrical shells, both without structural defects and with areas of a local adhesion failure, were determined numerically and experimentally. It is found that variations in the kinematic and static contact conditions on the interfaces of rigid layers of anisotropic elements of thin-walled structures considerably affects the character of distribution of transverse shear and compression strains. The model variant where the interfacial tangential and normal stresses on the contacting boundaries of layers are equal and their relative elastic slippage is allowed adequately reflects the behavior of layered thin-walled structures under large deformations.

## REFERENCES

1. E. I. Grigolyuk and P. P. Chulkov, *Stability and Vibrations of Three-Layer Shells* [in Russian], Mashinostroenie, Moscow (1973).
2. A. N. Guz', Ya. M. Grigorenko, I. Yu. Babich, et al., *Mechanics of Structural Elements. Mechanics of Composite Materials and Structural Elements in 3 Vols. Vol. 2* [in Russian], Naukova Dumka, Kiev (1983).
3. R. B. Rikards and G. A. Teters, *Stability of Shells of Composite Materials* [in Russian], Zinatne, Riga (1974).
4. D. V. Babich, "The effect of material delamination on the stability of orthotropic cylindrical shells," *Prikl. Mekh.*, **2**, No. 10, 52-56 (1988).
5. L. V. Andreev, I. P. Zhelezko, and N. I. Obodan, "On the bifurcation of equilibrium of spherical shells with delaminations," *Probl. Prochn.*, No. 2, 49-53 (1986).
6. V. V. Bolotin, "Defects of the delamination type in composite structures," *Mech. Compos. Mater.*, **20**, No. 2, 173-188 (1984).
7. B. Ya. Kantor, *Contact Problems of the Nonlinear Theory of Rotational Shells* [in Russian], Naukova Dumka, Kiev (1990).
8. A. N. Guz', *Damage Mechanics of Composite Materials in Compression* [in Russian], Naukova Dumka, Kiev (1990).
9. I. Yu. Babich and N. P. Semenyuk, "Stability and the initial postbuckling behavior of shells made of composites (review)," *Prikl. Mekh.*, **34**, No. 6, 3-38 (1998).
10. S. M. Vereshchaka, "To the discrete-structural theory of multilayer shells with structural defects," *Vest. NTU "KhPI"*, No. 31, 39-46 (2004).
11. V. V. Bolotin and Yu. N. Novichkov, *Mechanics of Multilayered Structures* [in Russian], Mashinostroenie, Moscow (1980).

12. K. Kerdward, E. Spier, and R. Arnold, "Stability of structural elements operating in compression," in: Prikl. Mekh. Kompoz.: Coll. Papers, 1986-1988 [Russian translation], Mir, Moscow (1989), pp. 8-57.
13. V. V. Vasil'ev, Mechanics of Structures of Composite Materials [in Russian], Mashinostrieniye, Moscow (1988).
14. G. A. Vanin and N. P. Semenyuk, Stability of Shells of Composite Materials with Imperfections [in Russian], Naukova Dumka, Kiev (1987).
15. N. P. Semenyuk and V. M. Trach, "Stability of cylindrical shells made of reinforced materials in axial compression with account of features of the layer-by-layer orientation of fibers," Prikl. Mekh., **42**, No. 3, 80-88 (2006).